Density Functional Theory Study of Transformations of Nitrogen Oxides Catalyzed by Cu-Exchanged Zeolites

ARTICLE *in* THE JOURNAL OF PHYSICAL CHEMISTRY B · APRIL 1998

Impact Factor: 3.3 · DOI: 10.1021/jp9734383

2 AUTHORS, INCLUDING:

William F Schneider
University of Notre Dame
205 PUBLICATIONS **4,362** CITATIONS

Density Functional Theory Study of Transformations of Nitrogen Oxides Catalyzed by Cu-Exchanged Zeolites

W. F. Schneider* and K. C. Hass

Ford Research Laboratory, MD 3083/SRL, Dearborn, Michigan 48121-2053

R. Ramprasad†

Department of Materials Science and Engineering, University of Illinois, Urbana, Illinois 61801

J. B. Adams

Department of Chemical, Bio and Materials Engineering, Arizona State University, Tempe, Arizona 85287

Received: October 23, 1997; In Final Form: January 30, 1998

A previously reported density-functional-theory-based model of NO decomposition in Cu-exchanged zeolites (Schneider, W. F.; et al. *J. Phys. Chem. B* **1997**, *101*, 4353) is extended to consider more generally the Cu-zeolite catalyzed chemistry of nitrogen oxides. The catalyst active site is considered to be an isolated, zeolite (Z)-bound Cu ion, which can exist in either a reduced (Z^-−Cu(I)) or an oxidized (Z^-−Cu(II)−O^-) state. Three different cluster models are used to study the affinity of ZCu and ZCuO for gaseous molecules (e.g., NO, NO_2, or N_2O), the structures and vibrational spectra of the stable complexes thus formed, and the possible reactivity between active sites and gaseous species. The reduced and oxidized states are found to react with nitrogen oxides via two types of O atom transfer reactions, one in which ZCu adds an O atom to form ZCuO, and the other in which ZCuO adds an O atom to form ZCu + O_2 via a dioxygen ($ZCuO_2$) intermediate. Potential energy surfaces for several key reactions are explored, and the results combined into a mechanistic model which can be used to rationalize much of the known catalytic chemistry of nitrogen oxides on Cu zeolites.

I. Introduction

Nitrogen oxides—ubiquitous byproducts of combustion—are key ingredients in a number of undesirable atmospheric processes, such as the generation of photochemical smog and of acid rain. Consequently, considerable effort has been expended in attempting to control their release, in particular through the use of catalysts that return the oxides to elemental nitrogen.[1] A variety of catalysts are known to effect this and other transformations of nitrogen oxides. Among these, Cu-exchanged zeolites, and in particular Cu−ZSM-5, exhibit the highest known activity for decomposition of NO to the elements (1)[2] and are also active for the decomposition of N_2O (2)[3] and the oxidation of NO to NO_2 (3).[4] The mechanisms of these

$$2\,NO \rightarrow N_2 + O_2 \quad (1)$$

$$N_2O \rightarrow N_2 + {}^1/_2O_2 \quad (2)$$

$$NO + {}^1/_2O_2 \leftrightarrow NO_2 \quad (3)$$

reactions remain to be fully elucidated, and in particular, in the case of reaction 1, have spurred considerable research and discussion.[5−11] Proposed mechanisms for reaction 1 have been surveyed elsewhere;[2] while the specifics vary, most involve diffusion of reactant molecules through the zeolite pores to isolated Cu-containing active sites, where the catalytic chemistry occurs. To assess such proposals, accurate microscopic descriptions of the active sites and reliable predictions of their reactivity are required. To date, spectroscopic and other laboratory studies have been the primary tools used to infer this information; more recently, however, atomistic models have begun to provide complementary insight into Cu zeolite catalyst chemistry.

In a high silica zeolite such as Cu−ZSM-5, exchanged Cu is believed to exist as isolated Cu(I) and Cu(II)[12] ions charge compensated by some combination of framework Al tetrahedral (T) sites[13] and extralattice species, such as O^-.[14,15] Electronic structure methods applied to simple cluster models of the zeolite-bound Cu ions have been quite successful in describing both the binding and coordination environment of Cu ions to the zeolite lattice and the structure, thermodynamics, and vibrational spectroscopy of Cu-bound species.[16,7c,17] An even more promising application of these models is to the prediction of chemical (catalytic) reactivity through the calculation of reaction pathways and barriers, but to date such investigations have been very limited.[16d,e] Using this approach, we recently proposed[16d] a mechanism for reaction 1 that involves the successive transfer of two oxygen atoms to a Cu ion bound near a single framework Al. Using the symbol Z to represent a formally monoanionic

* To whom correspondence should be addressed. E-mail: wschnei2@ford.com.

† Current address: Department of Physics and Astronomy, University of New Mexico, 800 Yale Blvd., NE, Albuquerque, New Mexico, 87131-1156.

S1089-5647(97)03438-X CCC: $15.00
Published on Web 04/22/1998

portion of the zeolite lattice, the mechanism can be summarized as follows:

$$ZCu + 2\ NO \rightarrow [ZCuONNO]^{\ddagger} \rightarrow ZCuO + N_2O \quad (4)$$

$$ZCuO + N_2O \rightarrow [ZCuOONN]^{\ddagger} \rightarrow ZCuO_2 + N_2 \quad (5)$$

$$ZCuO_2 \rightarrow ZCu + O_2 \quad (6)$$

The key catalytic intermediates in this model are ZCu, a zeolite bound Cu(I) ion, and ZCuO, a (nominally) Cu(II) ion charge compensated by both the zeolite and an extra-lattice oxygen. The ability to cycle between these states and thus to serve as an oxygen atom shuttle was identified as the key function of the Cu centers in the catalytic process. We present here a more complete density functional theory (DFT) examination of the binding, spectroscopy, and reactivity of nitrogen oxides with ZCu and ZCuO. The results allow us to propose a reaction scheme that accounts for the observed catalytic activity of the Cu zeolites and that is consistent with many experimental observations.

A central difficulty in applying electronic structure methods to the reactivity of Cu−zeolite catalysts is representation of the active site. ZSM-5, for instance, has a large (288 atom) unit cell containing a small number of nearly randomly distributed Al T-sites and associated Cu ions. The precise nature of the Cu environment, and its relationship to the observed reactivity, is unknown. A brute force approach to modeling this system is clearly impractical and, given the necessarily limited scope of such an approach, potentially misleading. In this and previous work we instead focus on obtaining a correct description of the Cu oxidation state and Cu−ligand (L) interactions and systematically study how these are modified by secondary zeolite coordination. In general, we find that a simple $(Cu-L)^+$ cluster (i.e., with the zeolite coordination ignored) correlates remarkably well with models containing sophisticated representations of the zeolite. In the present work, in addition to the $(Cu-L)^+$ model (**1a**), we examine two single T-site models in which the Cu ion

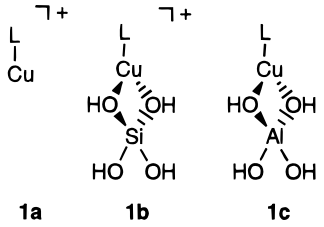

1a **1b** **1c**

is two-coordinated to $Si(OH)_4$ (**1b**) or $Al(OH)_4^-$ (**1c**). Previous theoretical[16a,b] and experimental work[18] is consistent with a low coordination environment for low valent Cu. These models are of a computationally convenient size, provide a reasonable representation of the zeolite coordination, and allow us to consider the effects of an environment ranging from very weakly to very strongly electron donating. All three models yield qualitatively similar results for nitrogen oxide binding and reactivity and differ quantitatively in chemically sensible ways. We believe that the use of models such as these, in which the coordination environment is varied in a rational manner, is ultimately the most efficient and productive route to modeling Cu−zeolite chemistry.

This paper is organized as follows. The computational approach is described in the following section. We then examine the binding modes, energetics, and vibrational spectroscopy of a range of small molecules coordinated to ZCu, including NO, N_2, O_2, CO, N_2O, and NO_2, followed by consideration of a similar series for ZCuO. Next we examine some reactions of these species with ZCu and ZCuO leading to cleavage of N−O and formation of N−N and O−O bonds. Finally, we combine these pieces into a mechanistic model of nitrogen oxide chemistry on Cu zeolite catalysts.

II. Computational Details

Energies and energy gradients were calculated using the Amsterdam Density Functional (ADF) code.[19] Geometries and vibrational spectra were determined within the local spin density approximation (LSDA)[20] and the final energies improved by perturbative application of Becke exchange[21] and Perdew correlation[22] gradient corrections (BP86). In previous studies of model Cu clusters, we have found that this approach gives results very similar to those obtained by the self-consistent application of gradient corrections in both the geometry optimization and energy calculation steps and that it is considerably more efficient computationally. A valence double-ζ plus polarization Slater-type basis was used for all atoms, save Cu, for which a double-ζ s and p and triple-ζ d Slater-type basis was used. The numerical integration mesh parameter, which determines the approximate number of significant digits in the internal numerical integrations in ADF, was set to at least 5.0, and in most cases 6.0.[19b] With these mesh parameters, total energies are converged to <0.1 kcal mol^{-1} and geometries to <0.001 Å. Geometry optimizations were performed in one of two ways: for simpler systems, the algorithms implemented in ADF were used directly, while for most of the larger T-site model calculations, the efficient natural internal coordinate and geometry optimization algorithms as implemented in GAMESS−US[25] were used. Geometries were converged to maximum and root-mean-square gradients of less than 10^{-4} and 4×10^{-5} hartree bohr^{-1}, respectively. Vibrational frequencies were obtained by two-sided numerical differentiation of the analytic gradients. In most cases all atoms were varied in the frequency evaluations, but in some the Z model was held fixed to reduce the number of gradient calculations necessary. Test calculations indicated essentially no difference in the vibrational frequencies obtained with either method. LSDA harmonic frequencies generally reproduce the experimental fundamentals of molecules within a few percent;[24] because this error is small but variable, we compare calculated vibrational frequencies directly with experimental results.

III. Results

Small Molecules. The calculated structures and harmonic vibrational frequencies of several key small molecules are listed in Table 1. The LSDA geometries agree very well with experiment. The LSDA harmonic frequencies overestimate the experimental fundamental frequencies by 0−6%, save for NO_3, in which case vibronic coupling strongly perturbs the e′ modes.[25] Mulliken populations and spin densities are reported for comparison with bound molecules and have unsurprising values. The binding energies reported in Table 1 and elsewhere are with respect to hypothetical, spin restricted atoms, and are meaningful only when combined to calculate the energies of chemical reactions.

ZCu Chemistry. Tables 2−4 contain calculated structural, energetic, and population data for the bare Cu^+, $Cu^+[Si(OH)_4]$, and $Cu^+[Al(OH)_4^-]$ models, respectively. Each of these is closed shell and formally d^{10}, but the Cu(I) center becomes progressively more electron rich across the series (compare, e.g., the Cu Mulliken charges). During geometry optimization,

TABLE 1: LSDA Structures,[a] Becke−Perdew Post-SCF Binding Energies,[b] Mulliken Charge and Spin Densities, and Vibrational Frequencies of Small Molecules[c]

	state	BE	geometry parameters[d]	Mulliken charges (spin densities)	vibrational frequency[d]
O	^3P	−35.6			
N_2	$^1\Sigma_g^+$	−378.5	N−N: 1.099 (1.098)		2408 (2331)
O_2	$^3\Sigma_u^-$	−220.7	O−O: 1.218 (1.207)		1568 (1556)
CO	$^1\Sigma^+$	−338.7	C−O: 1.131 (1.128)	C: 0.38	2180 (2143)
NO	$^2\Pi$	−277.0	N−O: 1.155 (1.151)	N: 0.26 (0.69)	1935 (1876)
				O: −0.26 (0.31)	
NO_2	$^2A_1$	−413.2	N−O: 1.197 (1.194)	N: 0.81 (0.45)	a_1: 754 (750)
			∠ONO: 133.4 (133.8)	O: −0.40 (0.27)	a_1: 1391 (1320)
					b_2: 1723 (1617)
N_2O	$^1\Sigma^+$	−482.6	N−N: 1.131 (1.127)	N_1: −0.16	π: 610 (589)
			N−O: 1.181 (1.185)	N_2: 0.62	σ^+: 1346 (1285)
				O: −0.46	σ^+: 2360 (2224)
NO_3	$^2A'_2$	−525.7	N−O: 1.231 (1.240)	N: 1.28 (−0.07)	e_1': 521 (380)
				O: −0.43 (0.36)	a_1': 793 (762)
					a_1': 1132 (1060)
					e_1': 1358 (1492)

[a] Distances in angstroms, angles in degrees. [b] Binding energy (kcal mol^{-1}) reported with respect to spin-restricted atoms. [c] Frequencies in cm^{-1}. [d] Experimental geometry and frequency data in parentheses diatomic data from ref. 36; polyatomic data as compiled in ref 25.

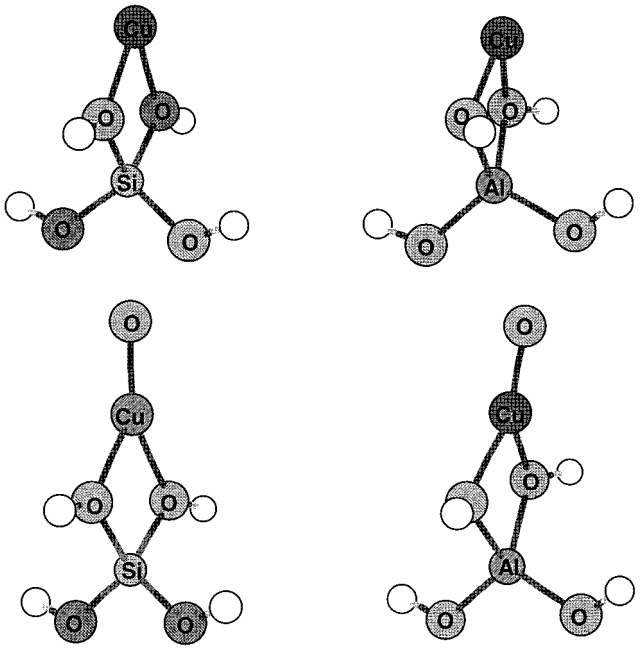

Figure 1. LSDA structures of ZCu (top) and ZCuO (bottom), for Z = $Si(OH)_4$ (left) and $Al(OH)_4^-$ (right). Open circles represent H atoms.

$Cu^+[Si(OH)_4]$ relaxes to a C_{2v} structure with a Cu−O separation of 2.01 Å, while the more strongly bound $Cu^+[Al(OH)_4^-]$ adopts a slightly puckered C_s conformation with a Cu−O separation of only 1.92 Å (Figure 1). The C_s $Cu^+[Al(OH)_4^-]$ structure is less than 1 kcal mol^{-1} more stable than a C_{2v}-constrained one, and presumably other conformations of similar energy and other or no symmetry also exist. The exact conformation of the T-site model has essentially no effect on the binding of additional molecules, and for computational convenience C_s symmetry is imposed in all the reported T-site model calculations. The framework structures shown in Figure 1 change very little with the addition of extralattice ligands.

ZCu can serve as a coordination center for a variety of gas molecules within a zeolite:

$$\mathrm{ZCu} + \mathrm{L} \leftrightarrow \mathrm{ZCuL} \qquad (7)$$

The simplest such adsorbates are the diatomics, including N_2, CO, NO, and O_2. While not directly relevant to nitrogen oxide chemistry, CO binding to Cu(I) has been used extensively as a spectroscopic probe of Cu−zeolite catalysts. N_2 binding is known but less widely studied.[10a,d] Isoelectronic CO and N_2 yield linear ZCu(I)−CO and ZCu(I)−N_2 complexes on all the ZCu models (Tables 2−4). CO bonding is accompanied by a slight decrease in C−O bond length and blue shift of C−O stretch frequency (Tables 1 and 5) and N_2 bonding by an increase in N−N separation and red shift of N−N frequency. The calculated C−O and N−N separations increase and stretch frequencies decrease as the Cu(I) center becomes more electron rich and is better able to back-donate π electron density to the ligand. The $Cu^+[Al(OH)_4^-]$ model reproduces surprisingly well the experimentally observed Cu(I)C−O and Cu(I)N−N vibrational frequencies in Cu−ZSM-5. As shown in Figure 2, CO binds by approximately 40 kcal mol^{-1} to ZCu, comparable to earlier predictions for CO on low-coordinate Cu(I),[16a] while apolar N_2 binds by only about 25 kcal mol^{-1}. The CO binding energy increases with the electron donating strength of the Z model, while N_2 binding has a smaller π component and is less sensitive to the Z model.

NO binding on Cu(I) in zeolites is well-known experimentally and has been studied extensively computationally.[16,17a−c] NO binds bent on ZCu, with an unpaired electron localized in an antibonding orbital of NO 2π origin. The bonding can thus be described as ZCu(I)−(·N═O) (i.e., with NO as a covalently bound neutral ligand).[16a] Similar to CO, NO is a strong π acid, and across the model series the Cu−N bond length decreases, the N−O bond length increases, the CuNO angle opens up, and the N−O stretch frequency shifts to the red, with the Z = $Al(OH)_4^-$ model giving the best agreement with the Cu(I)-NO vibrational frequency in Cu−ZSM-5. The ZCu−NO bond strength is slightly (3−6 kcal mol^{-1}) less than ZCu−CO in all models,[16a] with the smallest difference for electron-rich $Cu^+[Al(OH)_4^-]$ (Figure 2).

NO also binds O-down on ZCu, yielding a bent structure with an unpaired electron localized on the NO ligand (i.e., ZCu(I)−(O═N·)). The preference for N-down over O-down bonding ranges from 14 to 19 kcal mol^{-1} across the Z model series, with the difference least on the bare Cu^+ ion. While the O-down isomer is unlikely to be long lived, it is likely produced transiently and, as discussed below, may be an important intermediate in reactions involving O-atom transfer to Cu.

In addition to the mononitrosyls, NO readily forms dinitrosyls $ZCu(NO)_2$. In their most stable form, both NO ligands are

TABLE 2: LSDA Structures,[a] Becke−Perdew Post-SCF Binding Energies,[b] Mulliken Cu d Populations, Gross Charges, and Spin Densities of Bare Cu Models

		BE	selected geometry parameters						Cu d	Mulliken charges						Mulliken spin densities					
Cu^+		187.6							10.0	Cu:	1.00										
CuO^+	$^3\Sigma^-$	101.7	Cu−O:	1.728					9.47	Cu:	1.22	O:	−0.22			Cu:	0.35	O:	1.65		
CuO_2^+	$^3A''$	−49.0	Cu−O:	1.850	O−O:	1.231	CuOO:	118.6	9.77	Cu:	1.02	O_1:	−0.11	O_2:	0.09	Cu:	0.20	O_1:	0.73	O_2:	1.07
$Cu(\eta^2\text{-}O_2)^+$	$^3B_1$	−45.2	Cu−O:	2.010	O−O:	1.261	OCuO:	36.6	9.75	Cu:	1.08	O:	−0.04			Cu:	0.17	O:	0.91		
$CuNO^+$	$^2A'$	−124.0	Cu−N:	1.843	N−O:	1.139	CuNO:	128.6	9.73	Cu:	0.87	N:	0.25	O:	−0.12	Cu:	0.26	N:	0.42	O:	0.32
$CuON^+$	$^2A'$	−110.6	Cu−O:	1.937	N−O:	1.151	CuON:	128.9	9.83	Cu:	0.83	O:	−0.28	N:	0.45	Cu:	0.21	O:	0.15	N:	0.64
$CuCO^+$	$^1\Sigma^+$	−189.6	Cu−C:	1.818	C−O:	1.122	CuCO:	180.0	9.80	Cu:	0.86	C:	0.43	O:	−0.29						
CuN_2^+	$^1\Sigma^+$	−215.1	Cu−N_1:	1.831	N−N:	1.100	CuNN:	180.0	9.81	Cu:	0.91	N_1:	0.03	N_2:	0.05						
CuN_2O^+	$^1\Sigma^+$	−325.6	Cu−N_1:	1.817	N−N:	1.130	N_2−O:	1.156	9.83	Cu:	0.88	N_1:	−0.11	N_2:	0.53						
												O:	−0.30								
$CuON_2^+$	$^1A'$	−315.8	Cu−O:	1.894	O−N_1:	1.208	N−N:	1.118	9.90	Cu:	0.87	O:	−0.56	N_1:	0.73						
					$CuON_1$:	127.1	ONN:	−176.7				N_2:	−0.04								
$Cu(\eta^2\text{-}NO_2)^+$	$^2A'$	−244.4	Cu−N:	1.929	Cu−O_1:	2.116	O_1−N:	1.240	9.74	Cu:	0.94	N:	0.66	O_1:	−0.33	Cu:	0.29	N:	0.21	O_1:	0.31
			O_2−N:	1.172	O_1CuN:	35.3	O_1NO_2:	134.1				O_2:	−0.27					O_2:	0.19		
CuO_2N^+	$^2B_2$	−240.8	Cu−O:	1.937	O−N:	1.262	OCuO:	63.0	9.52	Cu:	1.06	N:	0.66	O:	−0.36	Cu:	0.38	N:	−0.04	O:	0.33
							ONO:	106.6													
$CuONO^+$	$^2A'$	−250.5	Cu−O_1:	1.856	O_1−N:	1.248	N−O_2:	1.166	9.82	Cu:	0.91	O_1:	−0.49	N:	0.84	Cu:	0.05	O_1:	0.22	N:	0.41
					CuO_1N:	119.1	O_1NO_2:	128.9				O_2:	−0.26					O_2:	0.32		
$CuNO_3^+$	$^2B_1$	−375.7	Cu−O:	1.939	O−N:	1.286	N−O′:	1.177	9.60	Cu:	1.10	N:	1.24	O:	−0.49	Cu:	0.34	N:	−0.04	O:	0.28
			OCuO:	66.1	CuON:	91.6	ONO′:	124.6						O′:	−0.35					O′:	0.13
$Cu(NO)_2^+$	$^1A_1$	−434.0	Cu−N:	1.936	N−O:	1.142	CuNO:	117.8	9.66	Cu:	0.76	N:	0.29	O:	−0.17						
							NCuN:	95.3													
$CuONNO^+$	$^3A''$	−409.6	Cu−O_1:	1.862	O_1−N_1:	1.204	N−N:	1.930	9.84	Cu:	0.88	O_1:	−0.42	N_1:	0.24	Cu:	0.12	O_1:	0.35	N_1:	0.85
							N_2−O_2:	1.127				N_2:	0.45	O_2:	−0.14			N_2:	0.37	O_2:	0.30
			CuO_1N_1:	122.1	$O_1N_1N_2$:	107.6	$N_1N_2O_2$:	111.3													
$[CuONNO^+]^‡$	$^3A''$	−380.1	Cu−O_1:	1.766	O_1−N_1:	1.605	N−N:	1.181	9.61	Cu:	1.02	O_1:	−0.47	N_1:	0.08	Cu:	0.24	O_1:	0.93	N_1:	0.07
(linear)							N_2−O_2:	1.173				O_2:	−0.27	N_2:	0.65			O_2:	0.45	N_2:	0.31
			CuO_1N_1:	111.9	$O_1N_1N_2$:	109.7	$N_1N_2O_2$:	159.5													
$[CuONNO^+]^‡$	$^3A''$	−374.9	Cu−O_1:	1.770	O_1−N_1:	1.651	N−N:	1.174	9.60	Cu:	1.02	O_1:	−0.44	N_1:	0.10	Cu:	0.25	O_1:	1.01	N_1:	0.03
(cyclic)			Cu−O_2:	2.979	O_2−N_2:	1.181						O_2:	−0.34	N_2:	0.66			O_2:	0.40	N_2:	0.31
			CuO_1N_1:	120.9	$O_1N_1N_2$:	109.9	$N_1N_2O_2$:	156.1													
			CuO_2N_2:	79.1	OCuO:	73.9															
$[CuOONN^+]^‡$	$^3A''$	−361.9	Cu−O_1:	1.779	O−O:	1.552	O_2−N_1:	1.397	9.64	Cu:	1.03	O_1:	−0.36	O_2:	−0.20	Cu:	0.22	O_1:	0.83	O_2:	0.41
(linear)							N_1−N_2:	1.132				N_1:	0.46	N_2:	0.07			N_1:	0.10	N_2:	0.44
			CuO_1O_2:	109.7	$O_1O_2N_1$:	117.0	$O_2N_1N_2$:	138.4													
$[CuOONN^+]^‡$	$^3A''$	−359.0	Cu−O_1:	1.855	O−O:	1.604	O_2−N_1:	1.272	9.57	Cu:	1.02	O_1:	−0.27	O_2:	−0.16	Cu:	0.35	O_1:	0.94	O_2:	0.17
(cyclic)					N−N:	1.172	N_2−Cu:	2.003				N_1:	0.52	N_2:	−0.11			N_1:	0.03	N_2:	0.51
			CuO_1O_2:	103.8	$O_1O_2N_1$:	111.7	$O_2N_1N_2$:	130.0													
$CuO\cdots ONO^+$	$^2A''$	−342.1	Cu−O_1:	1.719	O_1−O_2:	2.094	O_2−N:	1.157	9.56	Cu:	0.98	O_1:	−0.53	O_2:	−0.28	Cu:	0.22	O_1:	1.01	O_2:	−0.02
							N−O_3:	1.153				N:	1.09	O_3:	−0.26			N:	−0.13	O_3:	−0.08
			CuO_1O_2:	118.2	O_1O_2N:	118.0	O_2NO_3:	149.2													
$[CuOONO^+]^‡$	$^2A''$	−331.8	Cu−O_1:	1.762	O_1−O_2:	1.594	O_2−N:	1.305	9.60	Cu:	1.06	O_1:	−0.39	O_2:	−0.21	Cu:	0.22	O_1:	0.71	O_2:	0.08
							N−O_3:	1.159				N:	0.80	O_3:	−0.27			N:	−0.04	O_3:	0.03
			CuO_1O_2:	111.0	O_1O_2N:	117.5	O_2NO_3:	125.5													
$CuOO\cdots NO^+$	$^2A''$	−364.1	Cu−O_1:	1.832	O_1−O_2:	1.285	O_2−N:	1.948	9.78	Cu:	0.92	O_1:	−0.27	O_2:	−0.10	Cu:	0.06	O_1:	0.46	O_2:	0.50
							N−O_3:	1.110				N:	0.56	O_3:	−0.10			N:	−0.01	O_3:	−0.01
			CuO_1O_2:	112.3	O_1O_2N:	97.5	O_2NO_3:	102.0													

[a] Distances in angstroms, angles in degrees. [b] Binding energy (kcal mol^{-1}) reported with respect to spin-restricted atoms.

TABLE 3: LSDA Structures,[a] Becke−Perdew Post-SCF Binding Energies,[b] Mulliken Cu d Populations, Gross Charges, and Spin Densities of Z = $Si(OH)_4$ Models

		BE	Cu−O_F[c]	other selected geometry parameters						Cu d	Mulliken charges						Mulliken spin densities					
ZCu^+	$^1A_1$	−1024.7	2.013	Si−O_F:	1.694	O_FCuO_F:	72.6			9.94	Cu:	0.67										
$ZCuO^+$	$^3A''$	−1124.2	1.992	Cu−O:	1.698					9.38	Cu:	0.98	O:	−0.39			Cu:	0.45	O:	1.47		
$ZCuO_2^+$	$^3A''$	−1263.5	2.021	Cu−O_1:	1.804	O−O:	1.244	CuOO:	118.7	9.66	Cu:	0.81	O_1:	−0.15	O_2:	0.00	Cu:	0.24	O_1:	0.74	O_2:	1.00
$ZCu(\eta^2\text{-}O_2)^+$	$^3B_1$	−1264.8	1.993	Cu−O:	1.939	O−O:	1.280	OCuO:	38.6	9.60	Cu:	0.89	O:	−0.13			Cu:	0.29	O:	0.83		
$ZCuNO^+$	$^2A'$	−1336.0	2.005	Cu−N:	1.767	N−O:	1.158	CuNO:	139.9	9.63	Cu:	0.72	N:	0.16	O:	−0.22	Cu:	0.09	N:	0.54	O:	0.37
$ZCuON^+$	$^2A'$	−1320.3	2.015	Cu−O:	1.840	O−N:	1.172	CuON:	132.5	9.72	Cu:	0.70	O:	−0.34	N:	0.31	Cu:	0.03	O:	0.21	N:	0.77
$ZCuCO^+$	$^1A_1$	−1403.5	2.013	Cu−C:	1.778	C−O:	1.129	CuCO:	180.0	9.70	Cu:	0.61	C:	0.40	O:	−0.34						
$ZCuN_2^+$	$^1A_1$	−1428.6	2.011	Cu−N_1:	1.784	N−N:	1.104	CuNN:	180.0	9.70	Cu:	0.66	N_1:	0.03	N_2:	−0.03						
$ZCuN_2O^+$	$^1A_1$	−1535.4	2.025	Cu−N_1:	1.790	N−N:	1.130	N−O:	1.167	9.74	Cu:	0.63	N_1:	−0.07	N_2:	0.47						
													O:	−0.36								
$ZCuON_2^+$	$^1A_1$	−1523.2	2.035	Cu−O:	1.894	O−N_1:	1.201	N−N:	1.122	9.83	Cu:	0.61	O:	−0.53	N_1:	0.71						
						CuON_1:	126.2	ONN:	177.4				N_2:	−0.10								
$ZCu(\eta^2\text{-}NO_2)^+$	$^2A'$	−1461.6	1.997	Cu−N:	1.904	N−O_1:	1.260	N−O_2:	1.180	9.61	Cu:	0.77	N:	0.61	O_1:	−0.39	Cu:	0.34	N:	0.20	O_1:	0.26
			1.996	Cu−O_1:	1.996	O_1CuN:	37.3	O_1NO_2:	129.5						O_2:	−0.35					O_2:	0.14
$ZCuO_2N^+$	$^2B_2$	−1462.1	1.985	Cu−O:	1.933	O−N:	1.266	OCuO:	71.6	9.46	Cu:	0.87	O:	−0.42	N:	0.58	Cu:	0.46	O:	0.23	N:	−0.03
								ONO:	107.6												
$ZCuONO^+$	^2A	−1461.4	1.923	Cu−O_1:	1.814	O_1−N:	1.257	N−O_2:	1.175	9.66	Cu:	0.73	O_1:	−0.50	N:	0.76	Cu:	0.17	O_1:	0.22	N:	0.34
			2.180			CuO$_1$N$_1$:	119.8	O_1NO_2:	126.4						O_2:	−0.31					O_2:	0.26
$ZCuNO_3^+$	$^2B_2$	−1597.7	1.984	Cu−O:	1.934	O−N:	1.287	N−O′:	1.181	9.50	Cu:	0.90	O:	−0.53	N:	1.19	Cu:	0.44	O:	0.21	N:	−0.03
				OCuO:	66.4	CuON:	91.4	ONO′:	124.6						O′:	−0.42					O′:	0.07
$ZCu(NO)_2^+$	$^1A_1$	−1636.3	2.046	Cu−N:	1.894	N−O:	1.153	CuNO:	124.3	9.60	Cu:	0.63	N:	0.24	O:	−0.22						
								NCuN:	89.5												
$ZCuONNO^+$	$^3A''$	−1615.3	2.034	Cu−O_1:	1.833	O_1−N_1:	1.203	N−N:	1.851	9.75	Cu:	0.69	O_1:	−0.41	N_1:	0.21	Cu:	0.10	O_1:	0.38	N_1:	0.73
								N_2−O_2:	1.141				N_2:	0.39	O_2:	−0.20			N_2:	0.42	O_2:	0.36
				CuO$_1$N$_1$:	124.5	$O_1N_1N_2$:	107.6	$N_1N_2O_2$:	110.9													
[ZCuONNO$^+$]‡	$^3A''$	−1595.2	2.000	Cu−O_1:	1.745	O_1−N_1:	1.625	N−N:	1.178	9.49	Cu:	0.87	O_1:	−0.53	N_1:	0.03	Cu:	0.36	O_1:	0.86	N_1:	0.01
(linear)								N_2−O_2:	1.183				N_2:	0.60	O_2:	−0.34			N_2:	0.31	O_2:	0.40
				CuO$_1$N$_1$:	158.6	$O_1N_1N_2$:	63.7	$N_1N_2O_2$:	124.3													
[ZCuOONN$^+$]‡	$^3A''$	−1575.8	2.003	Cu−O_1:	1.751	O−O:	1.540	O_2−N_1:	1.360	9.51	Cu:	0.88	O_1:	−0.43	O_2:	−0.24	Cu:	0.33	O_1:	0.71	O_2:	0.26
(linear)								N−N:	1.145				N_1:	0.43	N_2:	−0.01			N_1:	0.12	N_2:	0.52
				CuO$_1$O$_2$:	110.1	$O_1O_2N_1$:	114.0	$O_2N_1N_2$:	135.5													
ZCuO···ONO$^+$	$^2A''$	−1552.0	2.008	Cu−O_1:	1.716	O_1−O_2:	1.901	O_2−N:	1.189	9.47	Cu:	0.95	O_1:	−0.56	O_2:	−0.31	Cu:	0.34	O_1:	0.89	O_2:	−0.03
								N−O_3:	1.169				N:	0.95	O_3:	−0.33			N:	−0.16	O_3:	−0.10
				CuO$_1$O$_2$:	108.7	O_1O_2N:	111.1	O_2NO_3:	136.8													
[ZCuOONO$^+$]‡	$^2A''$	−1549.1	1.992	Cu−O_1:	1.740	O_1−O_2:	1.621	O_2−N:	1.275	9.47	Cu:	0.90	O_1:	−0.46	O_2:	−0.24	Cu:	0.35	O_1:	0.59	O_2:	0.02
								N−O_3:	1.171				N:	0.76	O_3:	−0.33			N:	−0.03	O_3:	0.01
				CuO$_1$O$_2$:	108.1	O_1O_2N:	115.2	O_2NO_3:	125.1													
ZCuOO···NO$^+$	$^2A''$	−1570.1	2.022	Cu−O_1:	1.801	O_1−O_2:	1.299	O_2−N:	1.854	9.65	Cu:	0.78	O_1:	−0.30	O_2:	−0.15	Cu:	0.18	O_1:	0.42	O_2:	0.36
								N−O_3:	1.121				N:	0.51	O_3:	−0.16			N:	0.01	O_3:	0.01
				CuO$_1$O$_2$:	118.4	O_1O_2N:	99.1	O_2NO_3:	103.4													

[a] Distances in angstroms, angles in degrees. [b] Binding energy (kcal mol^{-1}) reported with respect to spin-restricted atoms. [c] Cu-framework oxygen distance.

TABLE 4: LSDA Structures,[a] Becke−Perdew Post-SCF Binding Energies,[b] Mulliken Cu d Populations, Gross Charges, and Spin Densities of Z = $Al(OH)_4^-$ Models

		BE	Cu−O_F[c]	other selected geometry parameters						Cu d	Mulliken charges						Mulliken spin densitiyes					
ZCu	$^1A'$	−1157.4	1.925	Al−O_F:	1.852	O_FCuO_F:	85.9			9.87	Cu:	0.50										
ZCuO	$^3A''$	−1271.2	1.924	Cu−O:	1.693					9.33	Cu:	0.94	O:	−0.54			Cu:	0.51	O:	1.28		
$ZCuO_2$	$^3A''$	−1400.9	1.934	Cu−O_1:	1.785	O−O:	1.262	CuOO:	121.2	9.55	Cu:	0.80	O_1:	−0.21	O_2:	−0.10	Cu:	0.33	O_1:	0.70	O_2:	0.89
$ZCu(\eta^2\text{-}O_2)$	$^3A'$	−1406.3	1.920	Cu−O:	1.937	O−O:	1.301	OCuO:	39.2	9.51	Cu:	0.87	O:	−0.20			Cu:	0.37	O:	0.75		
ZCuNO	$^2A'$	−1472.9	1.920	Cu−N:	1.734	N−O:	1.174	CuNO:	147.9	9.53	Cu:	0.72	N:	0.08	O:	−0.31	Cu:	0.07	N:	0.57	O:	0.37
ZCuON	$^2A'$	−1454.3	1.929	Cu−O:	1.808	O−N:	1.186	CuON:	137.2	9.60	Cu:	0.69	O:	−0.39	N:	0.19	Cu:	−0.03	O:	0.23	N:	0.82
ZCuCO	$^1A'$	−1537.0	1.925	Cu−C:	1.749	C−O:	1.141	CuCO:	179.9	9.59	Cu:	0.59	C:	0.33	O:	−0.41						
$ZCuN_2$	$^1A'$	−1561.0	1.927	Cu−N_1:	1.756	N−N:	1.112	CuNN:	179.7	9.60	Cu:	0.63	N_1:	−0.01	N_2:	−0.11						
$ZCuN_2O$	$^1A'$	−1663.7	1.938	Cu−N_1:	1.770	N−N:	1.133	N−O:	1.183	9.64	Cu:	0.61	N_1:	−0.07	N_2:	0.42						
						CuNN:	178.2	NNO:	179.8				O:	−0.43								
$ZCuON_2$	$^1A'$	−1648.9	1.949	Cu−O:	1.904	O−N_1:	1.196	N−N:	1.130	9.77	Cu:	0.54	O:	−0.53	N_1:	0.69						
						$CuON_1$:	124.9	ONN:	178.7				N_2:	−0.17								
$ZCu(\eta^2\text{-}NO_2)$	^2A	−1604.8	1.899	Cu−N:	1.863	N−O_1:	1.262	N−O_2:	1.196	9.52	Cu:	0.76	N:	0.54	O_1:	−0.43	Cu:	0.41	N:	0.14	O_1:	0.21
			1.932	Cu−O_1:	2.120	O_1CuN:	36.2	O_1NO_2:	126.1						O_2:	−0.43					O_2:	0.07
$ZCuO_2N$	$^2A''$	−1610.1	1.913	Cu−O:	1.968	O−N:	1.264	OCuO:	63.4	9.43	Cu:	0.82	O:	−0.48	N:	0.52	Cu:	0.49	O:	0.13	N:	−0.01
								ONO:	109.7													
ZCuONO	^2A	−1598.8	1.886	Cu−O:	1.802	O_1−N:	1.294	N−O_2:	1.190	9.52	Cu:	0.76	O_1:	−0.54	N:	0.61	Cu:	0.34	O_1:	0.20	N:	0.18
			1.974			CuO_1N:	121.2	O_1NO_2:	119.8						O_2:	−0.40					O_2:	0.12
$ZCuNO_3$	$^2A''$	−1744.7	1.912	Cu−O:	1.965	O−N:	1.283	N−O′:	1.194	9.46	Cu:	0.87	O:	−0.56	N:	1.154	Cu:	0.48	O:	0.14	N:	−0.02
				OCuO:	65.7	CuON:	91.0	ONO′:	123.8						O′:	−0.49					O′:	0.04
$ZCu(NO)_2$	$^1A'$	−1769.2	1.949	Cu−N_1:	1.859	N_1−O_1:	1.164	CuN_1O_1:	126.9	9.48	Cu:	0.66	N_1:	0.20	O_1:	−0.28						
				Cu−N_2:	1.876	N_2−O_2:	1.166	CuN_2O_2:	126.2				N_2:	0.17	O_2:	−0.28						
								NCuN:	88.2													
ZCuONNO	$^3A''$	−1743.4	1.935	Cu−O_1:	1.804	O_1−N_1:	1.214	N−N:	1.669	9.59	Cu:	0.73	O_1:	−0.43	N_1:	0.18	Cu:	0.24	O_1:	0.37	N_1:	0.47
								N_2−O_2:	1.168				N_2:	0.31	O_2:	−0.29			N_2:	0.43	O_2:	0.42
				CuO_1N_1:	129.8	$O_1N_1N_2$:	109.8	$N_1N_2O_2$:	113.8													
[ZCuONNO]‡	$^3A''$	−1736.7	1.921	Cu−O_1:	1.746	O_1−N_1:	1.653	N−N:	1.170	9.40	Cu:	0.88	O_1:	−0.59	N_1:	0.01	Cu:	0.44	O_1:	0.75	N_1:	−0.02
(linear)								N_2−O_2:	1.196				N_2:	0.54	O_2:	−0.42			N_2:	0.29	O_2:	0.32
				CuO_1N_1:	106.4	$O_1N_1N_2$:	110.3	$N_1N_2O_2$:	155.5													
[ZCuONNO]‡	$^3A''$	−1717.3	1.921	Cu−O_1:	1.754	O_1−O_2:	1.544	O_2−N_1:	1.334	9.42	Cu:	0.89	O_1:	−0.49	O_2:	−0.27	Cu:	0.41	O_1:	0.54	O_2:	0.14
(linear)								N−N:	1.157				N_1:	0.39	N_2:	−0.10			N_1:	0.14	N_2:	0.57
				CuO_1O_2:	108.5	$O_1O_2N_1$:	112.0	$O_2N_1N_2$:	133.9													
ZCuOO···NO	$^2A''$	−1702.0	1.926	Cu−O_1:	1.789	O_1−O_2:	1.331	O_2−N:	1.675	9.50	Cu:	0.83	O_1:	−0.37	O_2:	−0.19	Cu:	0.33	O_1:	0.32	O_2:	0.14
								N−O_3:	1.144				N:	0.44	O_3:	−0.26			N:	0.03	O_3:	0.03
				CuO_1O_2:	113.4	O_1O_2N:	103.7	O_2NO_3:	107.9													

[a] Distances in angstroms, angles in degrees. [b] Binding energy (kcal mol^{-1}) reported with respect to spin-restricted atoms. [c] Cu-framework oxygen distance.

TABLE 5: Selected Experimental and Calculated (LSDA) Stretching Vibrational Frequencies (cm^{-1}) for Nitrogen Oxides on Cu^+

		models			
		bare	$Si(OH)_4$	$Al(OH)_4^-$	exptl
$CuCO^+$	C−O	2263	2212	2138	2150−2160[a]
$CuNO^+$	N−O	1911	1881	1817	1810−1815[a]
CuN_2^+	N−N	2387	2350	2288	2295[b], 2156[c,d]
$Cu(\eta^2\text{-}O_2)^+$	O−O	1354[h]	1308	1247	
CuO_2^+	O−O	1433	1411	1346	
$Cu(NO)_2^+$	N−O asym	1927	1901	1844	1824−1827[a]
	N−O sym	1854	1773	1717	1729−1735[a]
$Cu(\eta^2\text{-}NO_2)^+$	N═O	1739[h]	1696	1633	1619−1635[c,e]
	N−O	1228	1205	1235	
$CuONO^+$	N═O	1739	1689	1613	1611−1643[c,f]
	N−O	1190	1115	965	
CuO_2N^+	NO_2 asym	1309	1321	1319	1300−1350[c,d]
	NO_2 sym	1025	1124	1212	
CuN_2O^+	N−N	2479	2453	2402	2230−2245[c,e,g]
	N−O	1441	1402	1345	
$CuNO_3^+$	N−O′	1608	1673	1657	1576−1607[c,f]
	NO_2 asym	1169	1193	1245	1305−1310[c,d]
	NO_2 sym	1001	1014	1035	
$[CuONNO^+]^‡$	TS-linear	647i	581i	526i	
	TS-cyclic	610i			
$[CuOONN^+]^‡$	TS-linear	1001i	855i	657i	
	TS-cyclic	642i			
$[CuOONO^+]^‡$	TS-linear	1031i	482i		

[a] See ref 16c. [b] References 10a,d. [c] Reference 6d. [d] Reference 7b. [e] Reference 11b. [f] Reference 37. [g] Reference 5a. [h] Saddle point.

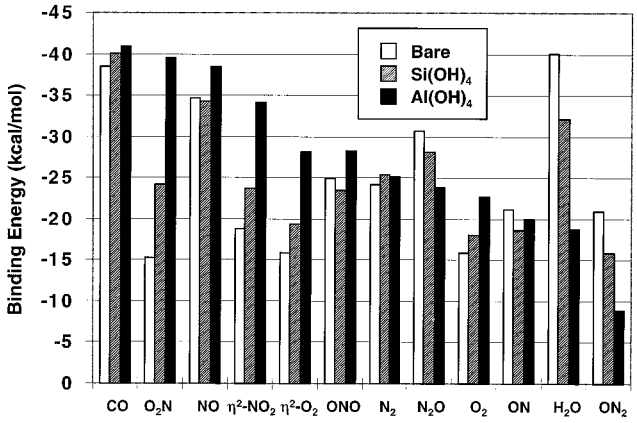

Figure 2. BP86 binding energies for a variety of adsorbates on ZCu.

N-bound to tetrahedral Cu to form a weakly coupled five-membered ring (**2**) which can be described in terms of the dative

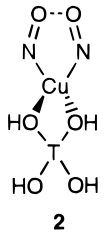

2

bonding of singlet-coupled $(NO)_2$ to ZCu.[16e] The triplet-coupled system has essentially the same structure but is several kcal mol^{-1} less stable. The second NO binds to ZCuNO by 33, 23, and 19 kcal mol^{-1} on bare Cu^+, $Cu^+[Si(OH)_4]$, and $Cu^+[Al(OH)_4^-]$, respectively, showing a relatively strong dependence on Z model and, by inference, on the electron density at the Cu center. Both symmetric and antisymmetric NO stretch modes are observed for the dinitrosyls, and as shown in Table 5, the splitting and absolute frequencies are well reproduced by the T-site models. Because of its ready formation and because it brings two NO ligands in close proximity, the dinitrosyl complex has often been proposed as an intermediate in N−N bond forming reactions:

$$ZCu + 2\ NO \rightarrow ZCu(NO)_2 \rightarrow ZCu + N_2 + O_2 \quad (8)$$

$$ZCu + 2\ NO \rightarrow ZCu(NO)_2 \rightarrow ZCuO + N_2O \quad (9)$$

Previous theoretical studies found no evidence for direct routes for reactions 8 or 9 on a Cu center.[16d,e]

While O_2 bonding to ZCu has been postulated[7] and desorption of molecular oxygen observed in temperature programmed studies,[26] direct spectroscopic evidence for $ZCuO_2$ remains lacking. We have identified two O_2 binding modes of comparable energy, the side-on, peroxide-like $ZCu(\eta^2\text{-}O_2)$ (**3a**), similar

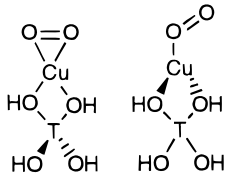

3a **3b**

to that reported by Trout et al.,[7c] and the end-on, superoxide-like $ZCuO_2$ (**3b**). Precedents for the latter bonding mode exist in the homogeneous chemistry of Cu(I) complexes with bulky polydentate ligands,[27] while the former is more typical of dinuclear Cu complexes. Both isomers have triplet ground states, and adsorption only slightly increases the O−O separation, suggesting a $ZCu(I)-O_2$ (or $ZCu(I)-\eta^2\text{-}O_2$) bonding description. The Cu center is more strongly oxidized by O_2 than by the other diatomics considered here, as indicated by the large Cu Mulliken charges and spin densities (Tables 2−4), and the bonding is better represented as a hybrid of $ZCu(I)-O_2$ and $ZCu(II)-O_2^-$. In the bare Cu^+ model, the bidentate isomer $Cu(\eta^2\text{-}O_2)^+$ is a saddle point 4 kcal mol^{-1} higher in energy than CuO_2^+. In the T-site models, in which the higher Cu oxidation state can be stabilized by square planar coordination about Cu, **3a** is lower in energy than **3b** by 1 and 5 kcal mol^{-1} for $Cu^+[Si(OH)_4]$ and $Cu^+[Al(OH)_4^-]$, respectively. Both isomers are true minima in the T-site models; we expect the bidentate isomer to dominate at room temperature in Cu-exchanged zeolites, with the equilibrium concentration of the superoxide isomer to increase with temperature. In the discussions that follow, we generically refer to both isomers as $ZCuO_2$.

The range of O_2 binding energies, from 16 to 28 kcal mol^{-1} (Figure 2), is somewhat greater than the low-temperature (<300 °C) molecular O_2 bonding energy inferred from experiment (11 kcal mol^{-1}),[26] but is consistent with the reversible adsorption of O_2 under mild conditions. The calculated $ZCu(\eta^2\text{-}O-O)$ and ZCuO−O stretch frequencies are strongly red-shifted compared to that of free O_2 and are predicted to occur in a region of the Cu−ZSM-5 spectrum close to that of lattice vibrational modes (Table 5), complicating their spectroscopic detection.

The triatomic adsorbates N_2O and NO_2 exhibit an even greater variety of coordination modes than the diatomics. N_2O preferentially binds N-down and linearly on all the ZCu models, forming $ZCu(I)-N_2O$. Bonding to electron-rich $Cu^+[Al(OH)_4^-]$ is relatively weak, and the structure of the bound ligand differs little from gaseous N_2O. In going to less electron rich $Cu^+[Si(OH)_4]$ and bare Cu^+, the $ZCu-N_2O$ bond energy increases and the N−N and N−O bond lengths decrease,

reflecting enhanced donation of antibonding electron density from the ligand to the Cu(I) center. These trends are strong and opposite those found for the diatomics, and as a result, N_2O cannot be placed unambiguously in a ZCu−L bond energies series: for example, a Cu^+ ion has a higher affinity for N_2O than for N_2, while for $Cu^+[Al(OH)_4^-]$ the opposite is true (Figure 2). Coordination to ZCu blue shifts both the "N−N" and "N−O" stretching modes, from 40 ($Cu^+[Al(OH)_4^-]$) to 120 cm^{-1} (Cu^+) for the former, compared to an observed blue shift of 6−21 cm^{-1} for N_2O adsorbed in Cu−ZSM-5 (Table 5). The absolute N−N stretch frequency is overestimated by upward of 150 to 250 cm^{-1}, comparable to the error observed for free N_2O in the LSDA (Table 1).

N_2O can also bind O-down and bent ($\angle$CuON $\approx$ 125°) on ZCu to produce $ZCuON_2$. This isomer is 10−15 kcal mol^{-1} less stable than the N-down form, and like the latter, binds most strongly to bare Cu^+. Like O-down NO, O-down N_2O is unlikely to be observed experimentally but may play a transient role in nitrogen oxide reactivity in Cu-exchanged zeolites.

At least three stable isomers of ZCu−NO_2 are possible, including the bidentate O-bound $ZCuO_2N$ (**4a**) and side-bound ZCu(η^2-NO_2) (**4b**), and the monodentate O-bound ZCuONO (**4c**). N-bound ($ZCuNO_2$, **4d**) is a true minimum energy

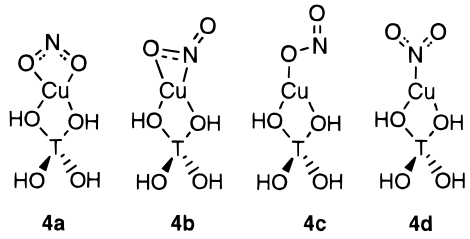

structure only in the bare Cu^+ model; in the T-site models with no symmetry constraints, **4d** relaxes without barrier to **4b**. We focus here on the first three isomers.

The NO_2 ligand is as strongly oxidizing as O_2, as revealed by the relatively high Cu charges, the low Cu d populations, and the even distribution of the doublet spin density between metal ion and ligand (Tables 2−4). The charge transfer is greatest in the symmetrically coordinated $ZCuO_2N$ isomer, which, like ZCu(η^2-O_2), is stabilized in the T-site models by square planar coordination about the Cu center. This charge transfer lengthens both N−O bonds compared to free NO_2, and produces a marked red shift of the asymmetric NO_2 stretch and a weaker red shift of the symmetric stretch. The charge transfer is also large in the side-on bound ZCu(η^2-NO_2) isomer. The Cu−N interaction is favored over the Cu−O one, producing a highly distorted square planar coordination about the Cu center in the T-site models, with the Cu−O framework bond *trans* to the Cu−N bond significantly shorter than the other. The Cu-bound O−N bond is lengthened and the free O−N bond shortened, and both N−O stretches are slightly red-shifted, compared to free NO_2. Finally, the Cu oxidation is least in the ZCuONO isomer, and the bonding in this case can be understood in terms of the Lewis description ZCu(I)−O−N═O; the N−O bond is lengthened and strongly red shifted, while the N═O bond is shortened and slightly blue shifted.

The relative stabilities of these isomers is sensitive to the local Cu^+ environment (Figure 2). The $CuONO^+$ isomer is most stable in the electron-poor bare Cu^+ model, with the $Cu(O_2N)^+$ isomer 8 kcal mol^{-1} higher in energy and the Cu(η^2-NO_2)$^+$ isomer a saddle point between $CuONO^+$ and $CuNO_2^+$. In contrast, in the electron-rich $Cu^+[Al(OH)_4^-]$ model the $ZCuO_2N$ isomer is lowest in energy, with ZCu(η^2-NO_2) and ZCuONO

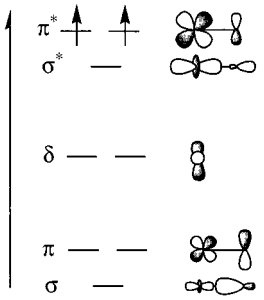

Figure 3. Schematic molecular orbital diagram for CuO^+.

isomers 5 and 11 kcal mol^{-1} higher in energy, respectively. The $Cu^+[Si(OH)_4]$ model is an intermediate case, in which the difference in energy between all three isomers is <1 kcal mol^{-1}. Based on these results, we expect the $ZCuO_2N$ and ZCu(η^2-NO_2) isomers to be the most stable in Cu-exchanged zeolites, with ZCuONO more likely existing as a short-lived intermediate. A number of bands in the vibrational spectrum of NO_2 in Cu-ZSM-5 have been assigned to bound NO_2, and these bands are consistent with those predicted here for $ZCuO_2N$ and ZCu(η^2-NO_2) (Table 5). The spectroscopic evidence is complex, however; and the assignments must be viewed with caution.

Finally, we note that Trout et al.[7c] have also examined the structures and stabilities of Cu-bound NO_2 at the LSDA level using a more complex Z model most resembling $Cu^+[Al(OH)_4^-]$. Surprisingly, they find the NO_2 geometry to be essentially unchanged from that of gas-phase NO_2 regardless of binding mode, and they calculate vibrational frequencies qualitatively inconsistent with those reported here or expected for an NO_2 ligand.[28] Further, they predict the relative stability to be $ZCuO_2N$ > $ZCuNO_2$ > ZCuONO, with energy differences in each case of 15 kcal mol^{-1}. It is rather unlikely that these gross qualitative differences with our results arise from different choices of Z models, and in fact we have been unable to reproduce the results of Trout et al.[7c] using Z models similar to theirs. We believe the results reported here more correctly represent NO_2 binding in Cu zeolite cluster models.

In summary, ZCu is predicted to reversibly bind a variety of gaseous species. Where experimental data is available and reliable, the calculated and observed vibrational spectra of the bound species are in reasonable agreement. Relative affinities of ZCu for adsorbates have been calculated and are shown in Figure 2 for all the adsorbates discussed above, plus H_2O for comparison, ordered by the binding energies obtained using the $Cu^+[Al(OH)_4^-]$ model. Adsorbates with a large dipolar component to bonding, or that strongly oxidize the Cu center, show large variability in binding energy, while more covalently bound species show little variability. The results provide some measure of the likely range of affinity within a real zeolite environment.

ZCuO Chemistry. ZCuO is the oxidized complement to an isolated ZCu.[7] As shown by the molecular orbital diagram for the parent CuO^+ (Figure 3), the Cu−O interaction is highly covalent, with both σ and π components that strongly mix Cu- and O-based orbitals. Double occupation of the π^* level produces a triplet ground state with a short (1.728 Å) and strong (50 kcal mol^{-1}) Cu^+−O bond. The corresponding open-shell singlet is about 15 kcal mol^{-1} higher in energy. Additional coordination (by, for example, $Si(OH)_4$ or $Al(OH)_4^-$) removes the rigorous orbital degeneracy but preserves the bonding description and, in particular, the triplet ground state. ZCuO can be represented in valence bond terms as a hybrid of ZCu(II)−$O^{\bullet -}$ and ZCu(I)−O(^{3}P), with the former resonance becoming progressively more favored with increasing Z donor

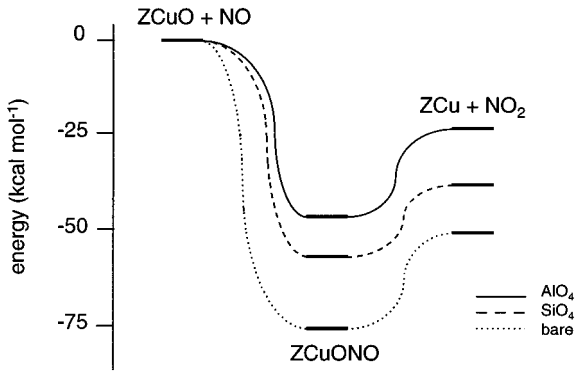

Figure 4. Potential energy surfaces for the reaction of ZCuO with NO.

strength. EPR spectroscopy has been used extensively to examine the oxidation state of Cu ions in active catalysts.[7a,11,14,29] It is important to note that, because of the presence of two unpaired electrons on adjacent centers, the EPR spectrum of ZCuO is unlikely to be comparable to that of isolated Cu(II) ions, and in practice may be unobservable. Care must be exercised in using EPR as a probe of catalyst oxidation state.

As shown in Figure 1, the ZCuO structures differ little from those of the corresponding ZCu. The ZCu−O bond shortens and increases in strength (to 64 and 78 kcal mol^{-1} for Z = $Si(OH)_4$ and $Al(OH)_4^-$, respectively) with added coordination. Because of its large binding energy, direct desorption of O(^{3}P) from ZCuO is unlikely to be an important reaction pathway. The calculated Cu−O stretch frequency ranges from 640 (Cu^+) to 725 ($Cu^+[Si(OH)_4]$) to 743 cm^{-1} ($Cu^+[Al(OH)_4^-]$). A band at 935 cm^{-1} in the infrared spectrum of oxidized Cu−ZSM-5 has been assigned to a Cu-extralattice O vibration;[30] more likely this band is associated vibrations of the zeolite lattice.[9a] Finally, we note that Trout et al.[7c] have also reported calculations for ZCuO, but apparently only considered a singlet, which we do not find to be the ground state.

Unlike ZCu, simple adsorption or desorption of gaseous species (reaction 10) is not a likely reaction motif for ZCuO.

$$ZCuO + L \longrightarrow ZCu(O)(L) \qquad (10)$$

Bare CuO^+ does bind species such as N_2, NO, and N_2O, but in each case the L−Cu−O angle is close to 180° and additional zeolite coordination at the Cu center destroys the Cu−L bonding. For example, a structure like that shown in reaction 10 has been proposed as the product of the addition of NO to ZCuO,[17b] and the N−O stretch frequency of "ZCuO(NO)" has even been assigned to a particular band in the infrared spectrum of NO on Cu−ZSM-5.[7b] We can find no evidence for a stable species with ZCuO(NO) connectivity, but find in this and all relevant additions to ZCuO that the O center is directly involved in the binding. We focus here specifically on the additions of NO and NO_2 to ZCuO; other transformations of nitrogen oxides on ZCuO are discussed in the following section.

We considered above the reaction of NO_2 with ZCu to produce various $ZCuNO_2$ isomers. The same products can be formed by the addition of NO to ZCuO. The addition can be envisioned to occur via an initially formed ZCuONO intermediate, which can subsequently isomerize or decompose. As shown in Figure 4, both routes to ZCuONO are barrierless and when combined provide a pathway for exchange of an O(^{3}P) atom between ZCu and NO (reaction 11). The entropic contribution

$$ZCuO + NO \leftrightarrow ZCu + NO_2 \qquad (11)$$

to reaction 11 is likely quite small, but overall energetics clearly favor the products over reactants, most so for bare Cu^+, but by 23 kcal mol^{-1} even for $Cu^+[Al(OH)_4^-]$. From the catalyst perspective, ZCuO can be reduced by NO to ZCu; equivalently, NO can extract an O(^{3}P) atom from ZCuO to form NO_2.

ZCuO is also able to add NO_2 to produce the nitrate $ZCuNO_3$ (reaction 12), which has a chelating structure[17b] and equivalent

$$ZCuO + NO_2 \longrightarrow ZCu(O)(O)N{-}O \qquad (12)$$

Cu−O bonds. NO_3 radical is unstable in the gas phase and is a strongly oxidizing ligand, producing in this case high charges and spin densities at the Cu center (Tables 2−4). $ZCuNO_3$ can thus be described as a hybrid between $ZCu(I)-NO_3^{\bullet}$ and $ZCu(II)-NO_3^-$, with the latter predominating. Reaction 12 is calculated to be exothermic by 64, 60, and 60 kcal mol^{-1} for bare Cu^+, $Cu^+[Si(OH)_4]$ and $Cu^+[Al(OH)_4^-]$, respectively. As shown in Table 5, the terminal N−O stretch frequency is insensitive to Z and is predicted to occur in a range similar to that observed in experiments; the NO_2 asymmetric stretch is more sensitive to Z, but is consistently lower in energy than bands assigned to this mode in Cu−ZSM-5.

ZCu ↔ ZCuO Transformations. To this point we have described a variety of ZCuL intermediates either known or likely to be produced in Cu-exchanged zeolites. A number of these play important roles in catalytic nitrogen oxide chemistry. A convenient way to analyze this chemistry is in terms of a coupling between a nitrogen oxide transformation and a formal O atom transfer to or from Cu (reactions 13 and 14, with the O

$$ZCu + O(^3P) \leftrightarrow ZCuO \qquad (13)$$

$$ZCuO + O(^1D) \leftrightarrow ZCuO_2 \qquad (14)$$

atomic state chosen to conserve electron spin). The oxidation of NO to NO_2 (reaction 11 and Figure 4) is one such example; the NO decomposition cycle (reactions 4−6) is another. Because ZCu is readily recovered from $ZCuO_2$ by desorption of O_2, ZCu, and ZCuO are seen to be the key intermediates in these transformations. Both reactions 13 and 14 are exothermic in the forward direction and thus provide a thermodynamic driving force for a coupled nitrogen oxide reaction; further, through this coupling, reaction pathways can be opened up which are otherwise energetically inaccessible. The net driving force of either reaction is a function of Z: Cu oxidation in reaction 13 is promoted by good electron donor environments, while Cu reduction in reaction 14 is promoted in poorly donating environments. In well-functioning catalysts, the coordination environment of an exchanged Cu ion within a zeolite may adjust during the course of a reaction to take advantage of these effects.

A good example of these principles is the reaction of two NO molecules to produce N_2O and an O(^{3}P) atom. Combining this reaction with reaction 13 yields reaction 4, which is

$$ZCu + 2\,NO \rightarrow [ZCuONNO]^{\ddagger} \rightarrow ZCuO + N_2O \qquad (4)$$

predicted to be exothermic by between 15 (bare Cu^+) and 42 (Z = $Al(OH)_4^-$) kcal mol^{-1}. The existence and nature of a microscopic pathway from reactants to products is not obvious. It is apparent that, if a transition state (TS) connecting reactants and products exists, it must incorporate the simultaneous formation of both N−N and Cu−O bonds. We identified four

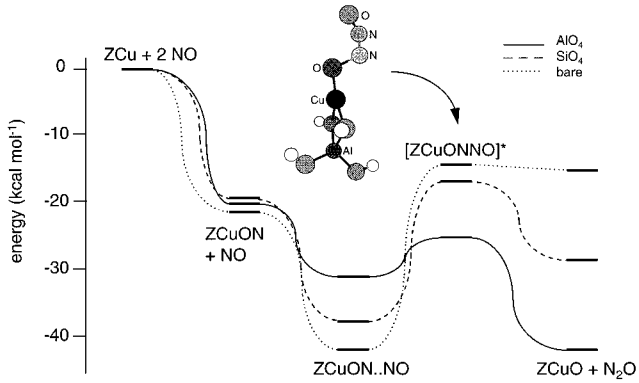

Figure 5. Potential energy surfaces for the reaction ZCu + 2 NO → ZCuO + N_2O.

candidate transition states meeting these criteria and located each on the $^3A''$ energy surface (**5a**−**d**, with the atoms forming N_2O highlighted). In general, the cis linear TS **5b** is lowest in energy, with the trans **5c**, the hyponitrite **5a**, and the four-membered cycle **5d** successively less stable. The structures and energies of **5b** in all three models are included in Tables 2-4, and the frequency along the reaction coordinate reported in Table 5. The three models give remarkably similar results for the TS structure, with the N−N bond nearly fully formed and N−O bond nearly completed cleaved.

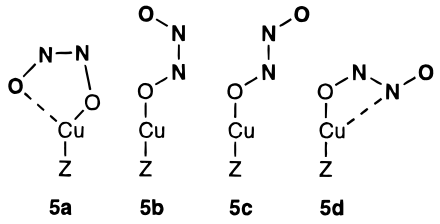

As shown in Figure 5, the TS is actually lower in energy than separated ZCu + 2 NO, reflecting the existence of at least one intermediate on the pathway leading to it. Using intrinsic reaction coordinate[31] (IRC) following, the entrance to the TS is found to be ZCuON···NO adduct with a large N−N separation—essentially a monodentate version of the O-down dinitrosyls reported previously—[16e]which is most likely formed by the addition of NO to ZCuON. Reaction 4 is thus predicted to proceed via formation of an activated O-down nitrosyl ZCuON, which reacts with a gas-phase NO in an Eley−Rideal process, passing first through the adduct and TS before reaching products.[16d] Neither ZCuNO nor $ZCu(NO)_2$ appears to play a direct role in this reactivity. While the ZCuON formation energy is essentially constant in all models, the relative stabilities of the adduct and TS track in opposite directions, so that the adduct is most stable and reaction barrier the greatest for bare Cu^+ and the adduct least stable and barrier the lowest for neutral $Cu^+[Al(OH)_4^-]$. Better estimates of the energetics await more sophisticated calculations. It is clear from these results that an energetically accessible route to reaction 4 exists, but not involving the intermediates traditionally invoked.

Conversion of N_2O to N_2 is in principle possible by coupling to either reaction 13 or 14. We consider the transfer of an $O(^1D)$ atom from N_2O to ZCuO first (reaction 5), since this reaction

$$ZCuO + N_2O \rightarrow [ZCuOONN]^{\ddagger} \rightarrow ZCuO_2 + N_2 \quad (5)$$

is spin-allowed. Again several related transition states can be located on the $^3A''$ energy surface. The lowest energy TS has a shape akin to **5b** (see Figure 6 and Tables 2−4): the N_2O molecule approaches the ZCuO site from the side and is rather substantially bent, the new O−O bond is partially formed, and the N_2−O bond is lengthened by about 0.2 Å along the way to being cleaved. The barrier height is lowest (19 kcal mol^{-1}) and overall energetics most favorable (−47 kcal mol^{-1}) in the electron-poor bare Cu^+ model. Both the barrier and overall energy become progressively less favorable in the more electron-rich $Cu^+[Si(OH)_4]$ (31 and −35 kcal mol^{-1}, respectively) and $Cu^+[Al(OH)_4^-]$ (36 and −26 kcal mol^{-1}, respectively) models. IRC following reveals a simple reaction coordinate, with the TS leading backward to separated reactants and forward to free N_2 and end-bound O_2. O_2 desorption recovers ZCu (Figure 6), with the overall ZCuO → $ZCuO_2$ → ZCu conversion ranging from thermoneutral (Z = $Al(OH)_4^-$) to exothermic by 31 kcal mol^{-1} (bare Cu^+).

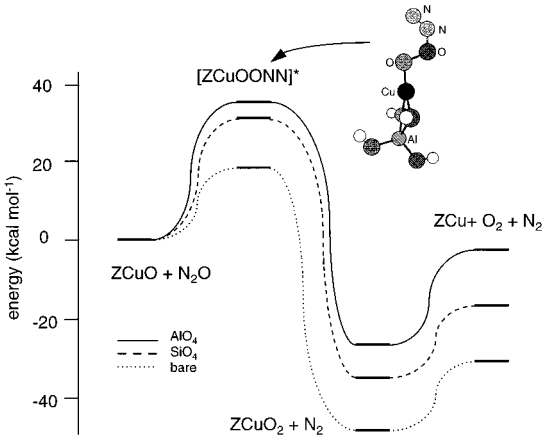

Figure 6. Potential energy surfaces for the reaction ZCuO + N_2O → ZCu + O_2 + N_2.

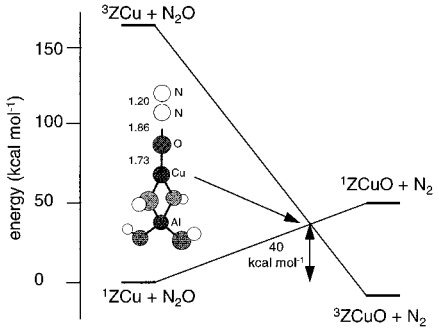

Figure 7. Schematic singlet and triplet potential energy surfaces for the spin-forbidden reaction ZCu + N_2O → ZCuO + N_2. Excited states shown are lowest energy states that preserve orbital symmetry.

A seemingly more likely pathway for reducing N_2O to N_2 is direct O atom transfer to ZCu (reaction 15). The net reaction

$$ZCu + N_2O \rightarrow [ZCuON_2]^{\ddagger} \rightarrow ZCuO + N_2 \quad (15)$$

energy is reasonable, ranging from 18 (bare Cu^+) to 5 (Z = $Si(OH)_4$) to −10 kcal mol^{-1} (Z = $Al(OH)_4^-$), but the reaction is spin forbidden, requiring the conversion of $O(^1D)$ from N_2O into $O(^3P)$ on ZCuO. Figure 7 contains an approximate state correlation diagram for the Z = $Al(OH)_4^-$ case, which shows that the separations of the singlet and triplet surfaces in the reactant and product geometries (160 and 60 kcal mol^{-1}, respectively) are quite large. Conceptually, the pathway for such a reaction is in part on the singlet surface and in part on the triplet, with the "transition state" the lowest point of intersection of the two; the probability of transferring from one surface to the other is controlled by spin−orbit coupling. The crossing

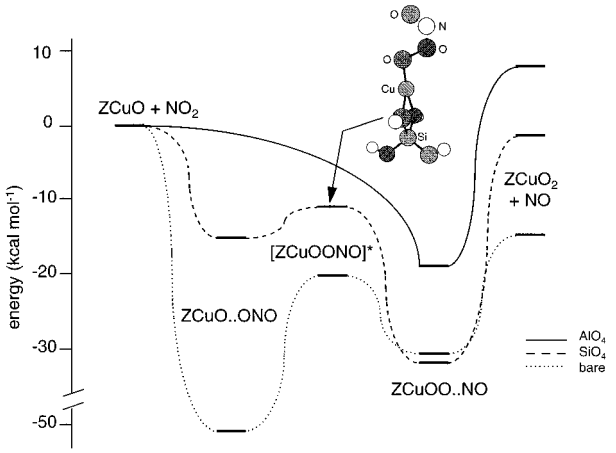

Figure 8. Potential energy surfaces for the reaction $ZCuO + NO_2 \rightarrow ZCuO_2 + NO$.

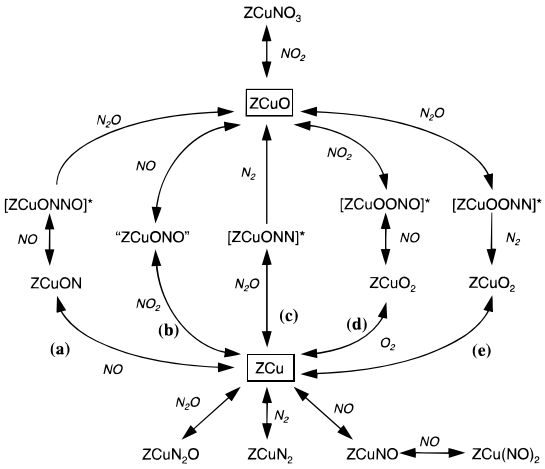

Figure 9. Combined reaction scheme. "ZCuONO" refers generically to all NO_2 isomers, which are presumed to be interconvertable.

point and spin−orbit coupling parameter for the related spin-forbidden dissociation of N_2O into $N_2 + O(^3P)$ have been studied in some detail.[32] A similarly detailed study is beyond the scope of the present work. We have performed manual searches for the lowest energy point of intersection of the singlet and triplet surfaces of $[Al(OH)_4^-]CuONN$, varying both the Cu−O and O−N separations while keeping the other coordinates fixed at reasonable values. To maintain the necessary control over electronic configurations, the search was restricted to C_{2v} structures. An intersection 40 kcal mol^{-1} above the reactants was located, 18 kcal mol^{-1} lower than that found in the N_2O study.[32] As expected from the crude state correlation diagram, the crossing is closer in structure to products than reactants, as was found in the N_2O dissociation case.[32] A more thorough search, in particular including reduced symmetry structures, may yield a lower energy intersection yet. These results are sufficient to conclude that the barriers to reactions 15 and 5 are comparable; the efficacy of spin−orbit coupling in reaction 15 will dictate how well it competes with ZCuO for N_2O.

We considered above the addition of NO_2 to ZCuO to form the nitrate $ZCuNO_3$ (reaction 12). An alternative channel for this reaction is the transfer of an $O(^1D)$ atom from NO_2 to ZCuO (reaction 16 and Figure 8), presumably proceeding through a

$$ZCuO + NO_2 \leftrightarrow [ZCuOONO]^{\ddagger} \leftrightarrow ZCuO_2 + NO \quad (16)$$

peroxy nitrite. The reaction is spin allowed and in our models ranges from somewhat exothermic (−14 kcal mol^{-1} for bare Cu^+) to slightly endothermic (+7 kcal mol^{-1} for $Cu^+[Al(OH)_4^-]$).

Reaction 16 provides the only example explored here in which the potential energy surface changes qualitatively with cluster model. The results are presented in Figure 8 and Tables 2−4. We searched the $^2A''$ surface for transition states for the O atom transfer, and for Cu^+ and $Cu^+[Si(OH)_4]$, we located structures resembling **5b** (Figure 8 and Tables 2 and 3). The two TSs have similar geometries and electronic structures, the forming O−O and cleaving N−O bonds 1.6 and 1.3 Å long, respectively, and the Cu oxidation states closer to ZCuO than $ZCuO_2$. The TS energies lie below both reactants and products, and further searching reveals even lower energy intermediates both in the entrance to (ZCuO···ONO) and exit from (ZCuOO···NO) the TS (Figure 8). These intermediates, like the ZCuON···NO intermediate identified in reaction 4, arise from relatively long-distance radical−radical interactions which are most pronounced in the cationic models (e.g., the dissociation energies of CuO^+···ONO and $[Si(OH)_4]CuOO^+$···NO are 53 and 30 kcal mol^{-1}, respectively). These interactions tend to diminish in importance in the neutral model. Thus, while both ZCuO···ONO and ZCuOO···NO intermediates are implicated for Cu^+ and $Cu^+[Si(OH)_4]$, only the latter exists for $Cu^+[Al(OH)_4^-]$, destabilized by ∼15 kcal mol^{-1}. As a result, the TS connecting the two intermediates in the Cu^+ and $Cu^+[Si(OH)_4]$ models does not exist in the $Cu^+[Al(OH)_4^-]$ one, and the formation of ZCuOO···NO from $ZCuO + NO_2$ in the last case occurs without barrier (Figure 8).

On the basis of these results alone, we cannot infer the molecular details of reaction 16 within a Cu−zeolite catalyst. Regardless of the details, reaction 16 is expected to be facile, given that the intermediates and transition states are lower in energy than the reaction endpoints in all models.

IV. Discussion of Catalytic Cycles

As the molecular binding results show, both ZCu and ZCuO form a variety of stable complexes with gas-phase nitrogen oxides, such as ZCuNO, $ZCuO_2N$, and $ZCuNO_3$. These complexes are expected to be long-lived at ambient temperatures, but at higher temperatures will tend to thermally dissociate, freeing ZCu and ZCuO to participate in the reactions described above. The detailed kinetics of these reactions are complicated by factors outside our models, such as the effect of the pore confinement on the gaseous species and the efficiency of energy redistribution between the active site and bulk lattice. We focus instead on the qualitative implications for Cu−zeolite catalysis. Figure 9 contains a reaction scheme which summarizes all the reactions discussed here. As we show below, the scheme can be used to rationalize the stoichiometric catalysis of reactions 1−3. Further, the scheme emphasizes the central role of direct and indirect (via $ZCuO_2$) conversions between ZCu and ZCuO intermediates, and makes evident the potential complications arising from competition between parallel reaction pathways.

NO Decomposition. Stoichiometric NO decomposition (reaction 1) is the most important and most speculated upon of the nitrogen oxide reactions catalyzed by Cu-exchanged zeolites. It is described within the reaction scheme by successive N−N (path a, reaction 4) and O−O (path e, reaction 5) bond forming reactions,[16d] yielding first N_2O and a Cu-bound O atom, then N_2 and Cu-bound O_2. While both reactions need not occur on the same Cu center, the zeolite may promote the overall reaction by restricting the diffusion of gas-phase N_2O from ZCuO, increasing the probability of their further reaction. Both bond-

forming steps have moderate barriers in the forward (clockwise in Figure 9) direction but much larger in the reverse, indicating that under moderate reaction conditions both steps should occur irreversibly. N_2O is observed to be formed when NO is passed over Cu−ZSM-5 at low temperatures,[5b,33] consistent with the N−N bond forming step occurring more readily than the O−O bond forming one.

Within this model, N−N bond formation is accommodated by a single, isolated Cu(I) ion, in agreement with both photoluminescence[14] and X-ray[18] spectroscopic evidence, and occurs by successive addition of two NO to the Cu(I) site. Previous experimental and theoretical studies have implicated either the mononitrosyl ZCuNO or the dinitrosyl $ZCu(NO)_2$ as the reactive intermediate for reaction 4;[7] in contrast, our results indicate that Cu and O centers must be adjacent for reaction to occur, and that this adjacency is most likely accomplished via a metastable isonitrosyl, ZCuON. Some workers have suggested that two proximal Cu(I) ions are necessary to catalyze N−N bond formation, either to produce N_2 and O_2 directly[5] (reaction 17) or to produce N_2O, with the remaining O atom shared

$$2\ ZCuNO \rightarrow 2\ ZCu + N_2 + O_2 \qquad (17)$$

$$2\ ZCu + 2\ NO \rightarrow Z_2[CuOCu] + N_2O \qquad (18)$$

between the two Cu as "Z_2[CuOCu]" (reaction 18).[9] The former proposal is unlikely based on our earlier studies of dinitrosyl chemistry.[16e] While we cannot rule out the participation of two ZCu centers in N_2O formation, we have demonstrated that two are not necessary. We are currently investigating the formation of Z_2[CuOCu] from ZCuO + ZCu to gain further insight into these Cu dimers. On basis of the results for reaction 4, however, if reaction 18 does occur, it will proceed via an isonitrosyl-like intermediate. Finally, others have proposed that N−N bond formation occurs via an intermediate like "$ZCu(NO)(NO_2)$" or "$ZCuN_2O_3$", which decomposes to yield N_2, O_2, and ZCuO.[6d,10a] We have not explicitly considered the higher nitrogen oxides in this work, but it is difficult to envision a pathway by which such a decomposition could occur. Our experience with the unstable "ZCuO(L)" coordination mode (reaction 10) suggests that highly coordinated, highly oxidized sites are unlikely intermediates.

The O−O bond-forming step in the stoichiometric NO decomposition mechanism involves reaction of a bound O atom (ZCuO) with N_2O to produce bound O_2 ($ZCuO_2$). O_2 is then desorbed to regenerate ZCu (reaction 6). This ability to cycle between oxidized (ZCuO) and reduced (ZCu) sites by successive O atom transfers, with the concomitant liberation of O_2, is central to all the mechanisms proposed here. Similar proposals have been advanced in the past;[7] a key contribution of this study is a molecular characterization of the oxidized and reduced states and identification of pathways between the two. While reduced "ZCu" and oxidized "ZCuO" states in Cu-exchanged zeolites are fairly well established experimentally, further experimental work is needed to verify the existence and O_2 lability of $ZCuO_2$. Inhibition of NO decomposition by excess O_2[5b,6b] can be explained within this scheme by its effect on the equilibrium between ZCu and $ZCuO_2$. O_2 may modify the reactivity in more subtle ways connected with the NO/NO_2 equilibrium, which we discuss below.

N_2O Decomposition. The description of stoichiometric N_2O decomposition (reaction 2) within the proposed reaction scheme also rests upon a ZCu/ZCuO cycle driven by successive O atom transfers. One step is shared with the NO decomposition mechanism (path e, Figure 9), while the other is the symmetry-forbidden transfer of an O atom from N_2O to ZCu (path c, reaction 15). The resultant catalytic cycle, obtained by traversing the two paths in a clockwise fashion in Figure 9, is similar to that previously advanced for Cu-exchanged zeolites, based on kinetic measurements.[3] The question of the identity of the "O" and "O_2" binding site was left open in the experimental work; our results show that ZCu can fulfill this role. O_2 also inhibits N_2O decomposition in Cu-exchanged zeolites,[3] an effect which again can be accounted for by its effect on the ZCu/$ZCuO_2$ equilibrium.

Paths c and e provide alternative pathways for the conversion of N_2O to N_2, and the two are expected to compete in functioning catalysts. The relative importance of the two is difficult to assess based on our results; within the limitations of our models, the two have roughly comparable barriers, with the former symmetry forbidden and thus further kinetically impeded. Cu−ZSM-5 activity for N_2O decomposition requires somewhat higher temperatures than does NO decomposition,[3,5b] suggesting that path e is favored over path c in this catalyst.

NO Oxidation. NO oxidation (reaction 3) differs from reactions 1 and 2 in that it has a moderate equilibrium constant over the temperature range of practical interest (300 to 600 °C), with the equilibrium shifting progressively toward reactants with increasing temperature.[6a] Cu−ZSM-5 is known to catalyze the approach to this equilibrium.[4] From a mechanistic viewpoint, it is most convenient to discuss reaction 3 in the reverse. In this direction, the reaction proceeds in a manner analogous to that of NO or N_2O decomposition: two O atoms are successively added from two NO_2 to a ZCu site, the first addition producing ZCuO and one NO (path b and reaction 11) and the second generating $ZCuO_2$ and a second NO (path d and reaction 16) via a "ZCuOONO" intermediate or transition state. A similar mechanism has been proposed for NO oxidation in the absence of a catalyst, with ZCu replaced by the second NO.[36] Neither catalyzed path is predicted to have an appreciable activation barrier, and in fact the unligated ZCu and ZCuO endpoints are the highest energy points along these pathways.

The most important consequence of the NO oxidation chemistry is its potential interference with other cycles between ZCu and ZCuO. Within the Cu cluster models, liberation of O_2 from two ZCuO sites (reaction 19) ranges from highly

$$2\ ZCuO \leftrightarrow 2\ ZCu + O_2 \qquad (19)$$

exothermic (−49 kcal mol^{-1} for bare Cu^+) to slightly endothermic (7 kcal mol^{-1} for $Cu^+[Al(OH)_4^-]$), with a significant entropic driving force at elevated temperatures. While Cu dimers may mediate reaction 19 in some circumstances, it is not clear how two O atoms can be combined from two well separated Cu centers. The NO oxidation pathways b and d provide one possible explanation: if these two are followed in parallel rather than in a cycle, the result is the NO catalyzed transport of O atoms between ZCuO sites (i.e., NO catalysis of reaction 19) and a short-circuit of the more desirable decomposition chemistry. A similar mechanism may also account for the observed "autoreduction" of Cu catalysts during thermal treatment, catalyzed by NO or possibly by other O atom acceptors, such as HO (to form HO_2).

The degree to which NO decomposition is affected by reaction 19 will be determined by the latter's equilibrium constant and rate. We expect the equilibrium to shift toward the right and to be approached more rapidly at higher temperatures. A distinguishing feature of both the catalytic decomposition and selective catalytic reduction of NO is the dropoff in activity above an optimal temperature.[2] A possible explana-

tion for this behavior is that, as the temperature increases, reaction 19 outcompetes the N_2O intermediates (path e) for the available ZCuO sites, shutting off the NO catalysis. Excess O_2 may inhibit decomposition in the opposite way, by driving reaction 19 to the left, and outcompeting paths a and c for ZCu. One suggestion for the role of hydrocarbons in promoting the selective catalytic reduction of NO_x is to offset this effect of O_2 and to restore a desirable balance between reduced and oxidized sites. Some experimental evidence is available to support this model.[35]

V. Conclusions

We have presented here a microscopically detailed model for Cu-exchanged zeolite catalytic activity toward nitrogen oxides. Because the Cu ions are essentially chemically independent in these catalysts, we employ a cluster description, focusing on the chemistry of a single, isolated ion. This approach has a number of important advantages: the models we use are small and readily tractable computationally, so that a wide range of chemistry can be investigated at a reliable level of theory; the influences on the chemistry are examined in a systematic manner, focusing first on the interactions of Cu ions with the nitrogen oxides, and then perturbations of these interactions by additional coordination; and the models are readily extensible. We use three different coordination models: bare Cu^+, $Cu^+[Si(OH)_4]$, and $Cu^+[Al(OH)_4^-]$, and find that, while the local coordination environment does modify the energetics of specific reactions, the qualitative chemistry is insensitive to the details of coordination.

The results support a description in which catalytic activity is associated with O atom transfers between the nitrogen oxides and reduced (ZCu) and oxidized (ZCuO) catalyst sites. Two types of O atom transfers are possible, the first converting ZCu to ZCuO, and the second ZCuO back to ZCu via a $ZCuO_2$ intermediate. Within this general framework, energetically plausible mechanisms for NO decomposition, N_2O decomposition, and NO oxidation can be identified. The key intermediates in the proposed mechanisms are not the stable complexes observed in many experiments, such as ZCuNO or $ZCuN_2O$, but rather are metastable species, such as ZCuON, $ZCuON_2$, and $ZCuO_2$, which may be difficult to observe in functioning catalysts. A prime justification for applying molecular models to this, or any, catalytic system is its ability to probe stable species and reactive intermediates with equal ease, counterbalancing the experimental bias toward the former.

Further work is clearly necessary to validate and extend the results presented here. We believe that these results provide a useful framework upon which to build a more complete, molecularly detailed understanding of the Cu zeolites catalysts, and hope that they inspire additional computational and experimental work in this scientifically and technologically important area.

Acknowledgment. The authors thank Bryan Goodman and Debasis Sengupta for numerous helpful discussions. Financial support for R.R. and J.B.A. through the Materials Research Laboratory program of NSF under contract 1-5-30897, by the National Center for Supercomputing Applications, and by Ford Motor Co. is gratefully acknowledged.

References and Notes

(1) Klimisch, R. L., Larson, J. G., Eds.; *The Catalytic Chemistry of Nitrogen Oxides*; Plenum: New York, 1975.

(2) (a) Shelef, M. *Chem. Rev.* **1995**, *95*, 209. (b) Iwamoto, M.; Hamada, H. *Catal. Today* **1991**, *10*, 57. (c) Centi, G.; Perathoner, S. *Appl. Catal., A* **1995**, *132*, 179.

(3) (a) Kapteijn, F.; Rodriguez-Mirasol, J.; Moulijn, J. A. *Appl. Catal., B* **1996**, *9*, 25. (b) Kapteijn, F.; Marban, G.; Rodriguez-Mirasol, J.; Moulijn, J. A. *J. Catal.* **1997**, *167*, 256.

(4) Shelef, M.; Montreuil, C. N.; Jen, H. W. *Catal. Lett.* **1994**, *26*, *277*.

(5) (a) Iwamoto, M.; Yahiro, H.; Mizuno, N.; Zhang, W.-X.; Mine, Y.; Furukawa, H.; Kagawa, S. *J. Phys. Chem.* **1992**, *96*, 9360. (b) Iwamoto, M.; Yahiro, H.; Tanda, K.; Mizuno, N.; Mine, Y.; Kagawa, S. *J. Phys. Chem.* **1991**, *95*, 3727.

(6) (a) Li, Y.; Hall, W. K. *J. Phys. Chem.* **1990**, *94*, 6145. (b) Li, Y.; Hall, W. K. *J. Catal.* **1991**, *129*, 202. (c) Hall, W. K.; Valyon, J. *Catal. Lett.* **1992**, *15*, 311. (d) Valyon, J.; Hall, W. K. *J. Phys. Chem.* **1993**, *97*, 1204. (e) Valyon, J.; Millman, W. S.; Hall, W. K. *Catal. Lett.* **1994**, *24*, 215. (f) Jang, H.-J.; Hall, W. K.; d'Itri, J. L. *J. Phys. Chem.* **1996**, *100*, 9416.

(7) (a) Larsen, S. C.; Aylor, A.; Bell, A. T.; Reimer, J. A. *J. Phys. Chem.* **1994**, *98*, 11533. (b) Aylor, A. A.; Larsen, S. C.; Reimer, J. A.; Bell, A. T. *J. Catal.* **1995**, *157*, 592. (c) Trout, B. L.; Chakraborty, A. K.; Bell, A. T. *J. Phys. Chem.* **1996**, *100*, 17582.

(8) (a) Shelef, M. *Catal. Lett.* **1992**, *15*, 305. (b)

(9) (a) Lei, G.-D.; Adelman, B. J.; Sárkány, J.; Sachtler, W. M. H. *Appl. Catal. B* **1995**, *5*, 245. (b) Beutel, T.; Sárkány, J.; Lei, G.-D.; Yan, J. Y.; Sachtler, W. M. H. *J. Phys. Chem* **1996**, *100*, 845.

(10) (a) Lamberti, C.; Salvalaggio, M.; Spoto, G.; Zecchina, A.; Geobaldo, F.; Vlaic, G.; Mellatreccia, M. *J. Phys. Chem. B* **1997**, *101*, 344. (b) Spoto, G.; Zecchina, A.; Bordiga, S.; Ricchiardi, G.; Martra, G.; Leofanti, G.; Petrini, G. *Appl. Catal. B*, **1994**, *3*, 151. (c) Spoto, G.; Bordiga, S.; Scarano, D.; Zecchina, A. *Catal. Lett.* **1992**, *13*, 39. (d) Spoto, G.; Bordiga, S.; Ricchiardi, G.; Scarano, D.; Zecchina, A.; Geobaldo, F. *J. Chem. Soc., Faraday Trans.* **1995**, *91*, 3285.

(11) (a) Anpo, M.; Matsuoka, M.; Shioya, Y.; Yamashita, H.; Giamello, E.; Morterra, C.; Che, M.; Patterson, H. H.; Webber, S.; Ouellette, S.; Fox, M. A. *J. Phys. Chem.* **1994**, *98*, 5744. (b) Giamello, E.; Murphy, D.; Magnacca, G.; Morterra, C.; Shioya, Y.; Nomura, T.; Anpo, M. *J. Catal.* **1992**, *136*, 510. (c) Sojka, Z.; Che, M.; Giamello, E. *J. Phys. Chem. B* **1997**, *101*, 4831.

(12) Throughout this work, we use the Cu(I) and Cu(II) notation to refer to the approximate oxidation state of Cu within a zeolite or a cluster model, and the superscript "+" symbol to denote the actual charge on a model cluster.

(13) (a) Schoonheydt, R. A. *Catal. Rev. Sci. Eng.* **1993**, *35*, 129. (b) Maxwell, I. E. *Adv. Catal.* **1982**, *31*, 1.

(14) (a) Dedecek, J.; Sobalík, Z.; Tvaruzková, Z.; Kaucky, D.; Wichterlová, B. *J. Phys. Chem.* **1995**, *99*, 16327. (b) Wichterlová, B.; Dedecek, J.; Vondrova, A. *J. Phys. Chem.* **1995**, *99*, 1065. (c) Dedecek, J.; Wichterlová, B. *J. Phys. Chem.* **1994**, *98*, 5721. (d) Wichterlová, B.; Dedecek, J.; Sobalík, Z.; Vondrova, A.; Klier, K. *J. Catal.* **1997**, *169*, 194.

(15) Sayle, D. C.; Catlow, C. R. A.; Gale, J. D.; Perrin, M. A.; Nortier, P. *J. Phys. Chem. A* **1997**, *101*, 3331.

(16) (a) Schneider, W. F.; Hass, K. C.; Ramprasad, R.; Adams, J. B. *J. Phys. Chem.* **1996**, *100*, 6032. (b) Hass, K. C.; Schneider, W. F. *J. Phys. Chem.* **1996**, *100*, 9292. (c) Ramprasad, R.; Schneider, W. F.; Hass, K. C.; Adams, J. B. *J. Phys. Chem. B* **1997**, *101*, 1940. (d) Schneider, W. F.; Hass, K. C.; Ramprasad, R.; Adams, J. B. *J. Phys. Chem. B* **1997**, *101*, 4353. (e) Ramprasad, R.; Hass, K. C.; Schneider, W. F.; Adams, J. B. *J. Phys. Chem. B* **1997**, *101*, 6903.

(17) (a) Yokomichi, Y.; Yamabe, T.; Ohtsuka, H.; Kakumoto, T. *J. Phys. Chem.* **1996**, *100*, 14424. (b) Trout, B. L. Chakraborty, A. K.; Bell, A. T. *J. Phys. Chem.* **1996**, *100*, 4173. (c) Zhanpeisov, N. U.; Nakatsuji, H.; Hada, M.; Nakai, H.; Anpo, M. *Catal. Lett.* **1996**, *42*, 173. (d) Blint, R. J. *J. Phys. Chem.* **1996**, *100*, 19518. (e) Brand, H. V.; Redondo, A.; Hay, J. P. *J. Phys. Chem. B* **1997**, *101*, 7691.

(18) Liu, D.-J.; Robota, J. in *Reduction of Nitrogen Oxide Emissions*, ACS Symposium Series 587; American Chemical Society: Washington, DC, 1995; p 147.

(19) (a) Baerends, E. J.; Ellis, D. E.; Ros, P. *Chem. Phys.* **1973**, *2*, 41. (b) Te Velde, G.; Baerends, E. J. *J. Comput. Phys.* **1992**, *99*, 84.

(20) Vosko, S. H.; Wilk, L.; Nusair, M. *Can. J. Phys.* **1980**, *58*, 1200.

(21) Becke, A. D. *Phys. Rev. A* **1988**, *38*, 3098.

(22) Perdew, J. P. *Phys. Rev. B* **1986**, *33*, 8822.

(23) Schmidt, M. W.; Baldridge, K. K.; Boatz, J. A.; Elbert, S. T.; Gordon, M. S.; Jensen, J. H.; Koseki, S.; Matsunaga, N.; Nguyen, K. A.; Su, S. J.; Windus, T. L.; Dupuis, M.; Montgomery, J. A. *J. Comput. Chem.* **1993**, *14*, 1347.

(24) (a) Fan, L.; Ziegler, T. *J. Chem. Phys.* **1992**, *96*, 9005. (b) Johnson, B. G.; Gill, P. M. W.; Pople, J. A. *J. Chem. Phys.* **1993**, *98*, 5612.

(25) Stirling, A.; Pápai, I.; Mink, J.; Salahub, D. R. *J. Chem. Phys.* **1994**, *100*, 2910.

(26) Valyon, J.; Hall, W. K. *J. Catal.* **1993**, *143*, 520.

(27) (a) Harata, M.; Jitsukawa, K., Masuda, H.; Einaga, H. *J. Am. Chem. Soc.* **1994**, *116*, 10817. (b) Wei, N.; Murthy, N.; Chen, Q.; Zubieta, J.; Karlin, K. D. *Inorg. Chem.* **1994**, *33*, 1953. (c) Kitajima, N.; Moro-oka, Y. *Chem. Rev.* **1994**, *94*, 737. (d) Karlin, K. D.; Gultneh, Y. *Progress Inorganic Chemistry* Lippard, S. J., Ed.; Wiley: New York, 1987; Vol. 35.

(28) Nakamoto, K. *Infrared and Raman Spectra of Inorganic and Coordination Compounds*, 4th ed.; Wiley: New York, 1986.

(29) (a) Kucherov, A. V.; Gerlock, J. L.; Jen, H.-W.; Shelef, M. *J. Phys. Chem.* **1994**, *98*, 4892. (b) Kucherov, A. V.; Gerlock, J. L.; Jen, H.-W.; Shelef, M. *Catal. Today* **1996**, *27*, 79.

(30) Valyon, J.; Hall, W. K. *J. Phys. Chem.* **1993**, *97*, 7054.

(31) Schlegel, H. B. *Adv. Chem. Phys.* **1987**, *67*, 249.

(32) Chang, A. H. H.; Yarkony, D. R. *J. Chem. Phys.* **1993**, *99*, 6824.

(33) Li, Y.; Armor, J. N. *Appl. Catal.* **1991**, *76*, L1.

(34) Bhatia, S. C.; Hall, J. H., Jr. *J. Phys. Chem.* **1980**, *84*, 3255.

(35) (a) Cho, B. K. *J. Catal.* **1993**, *142*, 418. (b) Cho, B. K. *J. Catal.* **1995**, *155*, 184.

(36) Huber, K. P.; Herzberg, G. *Molecular Structure and Molecular Spectra. IV. Constants of Diatomic Molecules*; Van Nostrand Reinhold: Toronto, 1979.

(37) Hoost, T. E.; Laframboise, K. A.; Otto, K. *Catal. Lett.* **1995**, *33*, 105.